

Special Feature: Analysis Techniques to Evaluate the Next Generation Electronic Materials

Research Report

Local Atomic Structure Analysis of SiO₂/SiC Interfaces Using X-ray Absorption Spectroscopy

Noritake Isomura, Takamasa Nonaka and Yukihiro Watanabe

Report received on Dec. 3, 2018

■ABSTRACT■ Material interfaces occur in all semiconductor devices, and their exact structure is a key determinant of device performance. However, it is usually not straightforward to analyze the exact composition of interfacial structures in a layer-by-layer manner. Here, local atomic structure analysis of the interface between chemical-vapor-deposited SiO₂ and SiC (4H, m-face) is achieved by a combination of chemical-state-selective extended X-ray absorption fine structure (EXAFS) spectroscopy and a thinned SiO₂ film sample. The chemical-state-selective Si K-edge EXAFS measurements of SiO₂ and SiC are achieved by the detection of bond-specific Auger electrons, using the differential electron yield (DEY) mode. EXAFS spectroscopy can be used to determine interatomic distances and coordination numbers from the spectral oscillations caused by photoelectron scattering. The Fourier transform derived from the oscillations of the SiC-selective DEY-EXAFS spectrum shows an intensity reduction (17%) of the first-nearest-neighbor peak with respect to bulk SiC, suggesting that carbon vacancy defects could exist on the SiC side of the SiO₂/SiC interface. On the other hand, the Si–O distance determined from the SiO₂-selective DEY-EXAFS spectrum was 1.57 Å, suggesting that the SiO₂ side adopts a structure close to that of tridymite.

■KEYWORDS■ SiC-MOS, SiO₂, Interface, EXAFS, Auger Electron

1. Introduction

Material interfaces are present in all semiconductor devices, and their exact structure strongly influences device performance. Recently, silicon carbide (SiC), which possesses high chemical and thermal stability as well as high dielectric breakdown strength, has been recognized as the material for next-generation power semiconductor devices. However, in contrast to silicon, the interface between silicon dioxide (SiO₂) and SiC is not ideal in the respect that a high density of states at the interface originating from a high concentration of defects deteriorates the performance of metal–oxide–semiconductor (MOS) devices.⁽¹⁻⁴⁾ The nature of these interface defects is under debate.⁽⁵⁻¹⁴⁾

X-ray absorption spectroscopy (XAS), which provides information about the local atomic structure, has been widely used for various materials. In particular, extended X-ray absorption fine structure (EXAFS) spectroscopy can be used to determine interatomic distances and coordination numbers from the spectral oscillations caused by photoelectron scattering.⁽¹⁵⁾ However, the interface cannot be selectively probed in

typical measurements.

We previously reported a method for local atomic structure analysis of the interface between SiO₂ and SiC on the SiC-side using EXAFS spectroscopy.⁽¹⁶⁾ The schematic principle is shown in **Fig. 1**. This method

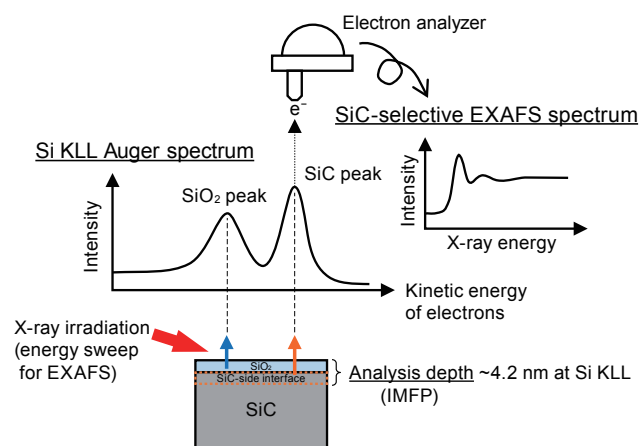


Fig. 1 Schematic showing the principle of the measurement method for the SiC-side interface between SiO₂ and SiC using EXAFS spectroscopy.

combines the following two ideas: (1) with a SiO₂ film thinner than the analysis depth, Auger electrons originating from the interface can be detected as they can pass through the SiO₂ film; (2) measurements can be tuned to SiC by detecting Auger electrons originating from the SiC layer through monitoring the SiC-assigned Si KLL peak in the Auger electron spectroscopy (AES) spectra, as recorded in the Auger electron yield (AEY) mode.^(17,18)

In the AEY mode, which records the intensity of an Auger peak at a fixed electron energy, the intensity increases locally in the narrow energy region where the photoelectron peaks cross during an energy sweep of the incident X-ray, resulting in the modification of the EXAFS spectrum. In the case of SiO₂/SiC, photoelectron peaks such as C 1s and O 1s cross within the EXAFS oscillation. The differential electron yield (DEY) mode can remove this photoelectron crossing by subtracting it as the background, enabling EXAFS measurements in the AEY mode.⁽¹⁹⁾ By using the DEY mode, chemical-state-selective EXAFS measurements, which separate multiple chemical states at the time of measurement, become feasible.

In the present study, we demonstrate that the local atomic structures of not only the SiC side but also the SiO₂ side of a SiO₂/SiC interface can be obtained. The SiO₂-side interface, with a thin SiO₂ film, was obtained by etching and was measured by monitoring the Si KLL peak assigned to SiO₂.⁽²⁰⁾ To demonstrate this EXAFS method, a SiO₂ film prepared by chemical vapor deposition (CVD) was used because a thermally oxidized film can cause complexity at the interface due to the oxidation process.

2. Experimental

The experiments were conducted at the XAS beamline BL6N1 of the Aichi Synchrotron Radiation Center (AichiSR),^(21,22) which has an electron storage ring with a circumference of 72 m and is operated at an electron energy of 1.2 GeV and a current of 300 mA. White light from a bending magnet, ranging from 1750 to 6000 eV, was monochromatized by an InSb(111) double-crystal monochromator for the Si K-edge. The energy resolution, $E/\Delta E$, is approximately 2000 at 3000 eV. The beam size at the sample position was ~ 2 mm \times ~ 1 mm (horizontal \times vertical).

The electron analyzer (SPECS PHOIBOS 150) used in this study can operate up to kinetic energies of

3500 eV. It comprises a hemispherical energy analyzer with a mean radius of 150 mm; a pre-retarding, combined, second-order focusing-lens system; and a two-dimensional event-counting detector equipped with a multichannel plate, a phosphor screen, and a charge-coupled device camera. The pass energy was set to 10 eV. The base pressure of the main chamber was approximately 5×10^{-8} Pa.

The X-ray beam from the beamline was horizontally incident and horizontally polarized. The axis of the input lens of the analyzer (acceptance angle = $\pm 5^\circ$) was parallel to the polarization vector, and the angle between the axis and the incident beam was 54° . For the DEY-EXAFS measurements, electrons emitted normal to the sample surface were detected using an electron analyzer during X-ray energy sweeps (take-off angle (TOA) = 90°). For the total electron yield (TEY) measurements, which were performed as bulk-sensitive measurements for comparison, the sample drain current was measured.

The sample comprised SiO₂ (3.7 nm)/SiC(4H, m-face). The SiO₂ film was deposited by low-pressure CVD followed by annealing in nitrogen (N₂) at 1300°C under ambient pressure. The SiO₂ film was then thinned to 3.7 nm by etching in a hydrogen fluoride solution. The thickness was measured using an ellipsometer (Gaertner Scientific L115C). A thick, thermally oxidized SiO₂ film and a bulk SiC sample were also tested for comparison (referred to as “bulk SiO₂” and “bulk SiC,” respectively).

3. Results and Discussion

Figure 2 shows the X-ray photoelectron spectroscopy

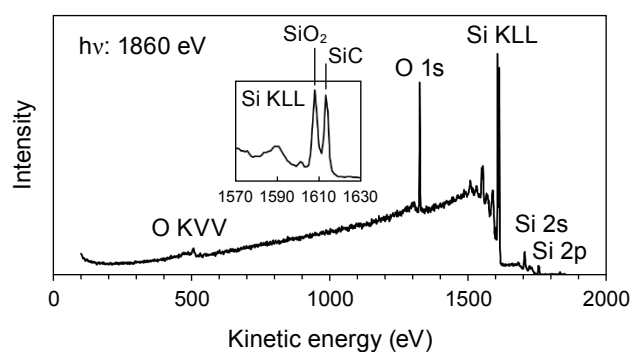


Fig. 2 XPS spectrum of the SiO₂/SiC sample surface at a photon energy of 1860 eV. The SiO₂ film is 3.7 nm thick. The inset shows an enlarged view of Si KLL.

(XPS) spectrum of the SiO_2/SiC sample surface under irradiation at a photon energy (hereafter “PE”) of 1860 eV. Auger and photoelectron peaks that are assigned to the Si and O elements in the sample were observed. The Si KLL spectrum shows two Auger peaks at 1608.2 eV and 1613.4 eV, which are assigned to SiO_2 and SiC, respectively.⁽²³⁾ The SiO_2 - and SiC-assigned Auger and background intensities were monitored at kinetic energies (hereafter “KEs”) of 1608.2 eV, 1613.4 eV, and 1633.4 eV, respectively, during X-ray energy sweeps for DEY-EXAFS measurements.

The SiC- and SiO_2 -assigned Auger and background EXAFS spectra are shown in Fig. 3. The intensities were normalized by the incident X-ray intensities, which were determined using the current of an Al mesh inserted in the path of the X-ray beam. As can be seen, the Si K-edge was observed at the PE of 1850 eV in the Auger EXAFS spectrum but not in

the background spectrum. In both spectra, two peaks due to the photoelectron crossing of C 1s and O 1s were observed. In Fig. 3(a), for SiC, the positions of these peaks in the background EXAFS spectrum were shifted toward higher KE (by 20.0 eV) compared with those in the Auger EXAFS spectrum. This is because the energy window for the background (1633.4 eV) was placed at a 20.0 eV higher than that of the Auger energy (1613.4 eV), and the photoelectron peaks crossed each energy window at KEs that differed from each other by 20.0 eV. On the other hand, for SiO_2 , the difference is 25.2 eV for the SiO_2 -assigned and background EXAFS spectra, as shown in Fig. 3(b).

The SiC- and SiO_2 -selective DEY-EXAFS spectra were obtained by subtraction of the background spectra from the SiC- and SiO_2 -assigned Auger EXAFS spectra, respectively, and are shown in Fig. 4 along with the TEY-EXAFS spectra of bulk SiC and

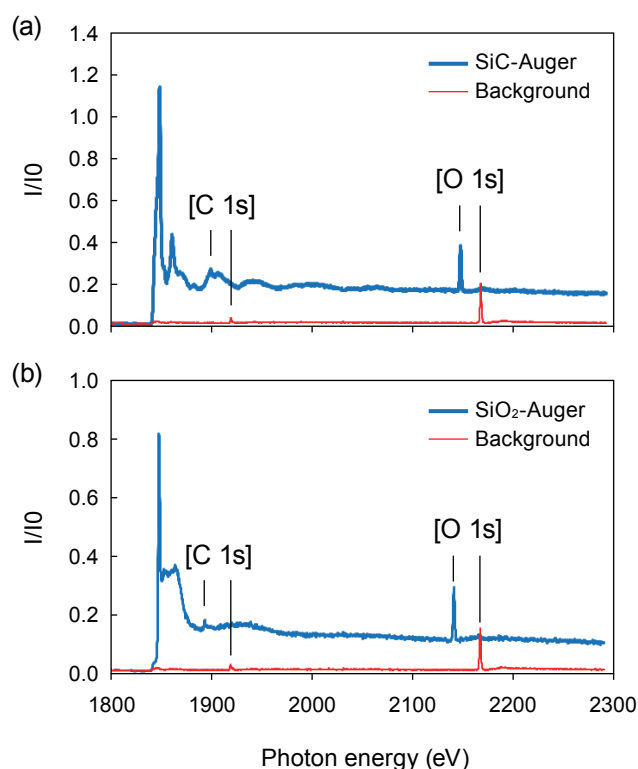


Fig. 3 Si K-edge EXAFS spectra measured at different Si KLL Auger peaks ((a) SiC and (b) SiO_2 , 1613.4 eV and 1608.2 eV, respectively, blue) and background (1633.4 eV, red). The brackets indicate the peaks caused by photoelectrons crossing over the electron energy windows for the Auger and background spectra.

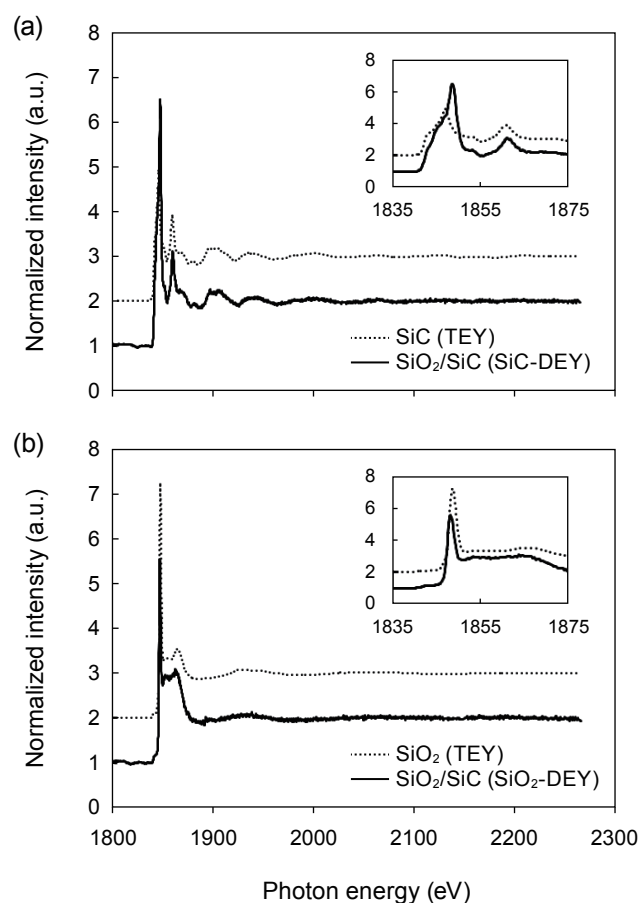


Fig. 4 (a) EXAFS spectra of SiO_2/SiC (SiC-selective DEY) and SiC (TEY) and (b) EXAFS spectra of SiO_2/SiC (SiO_2 -selective DEY) and SiO_2 (TEY). The insets show enlarged views of the XANES regions.

SiO₂ samples for comparison. The subtractions were performed after shifting the background EXAFS spectra to lower KEs by 20 eV and 25.2 eV for SiC and SiO₂, respectively, following the procedure for DEY-EXAFS analysis.⁽²⁰⁾ The peaks due to the photoelectron crossing of C 1s and O 1s were removed. In addition to the Si K-edge at 1850 eV, EXAFS oscillations were observed in both DEY-EXAFS spectra, which were similar to those in the TEY-EXAFS spectra. However, in the X-ray absorption near-edge structure (XANES) region,⁽²⁴⁾ ranging from 1840 to 1845 eV, the SiC DEY spectrum differed from the TEY spectrum (XANES modification), although the DEY and TEY spectra are similar for SiO₂, as shown in the insets of Fig. 4.

Figure 5 shows the Si KLL Auger spectra under irradiation at various PEs in the XANES region. The peaks at KEs of 1608.2 eV and 1613.4 eV indicate SiO₂ and SiC, respectively. The strong peak at a KE of 1612.7 eV was observed only at a PE of 1848 eV,

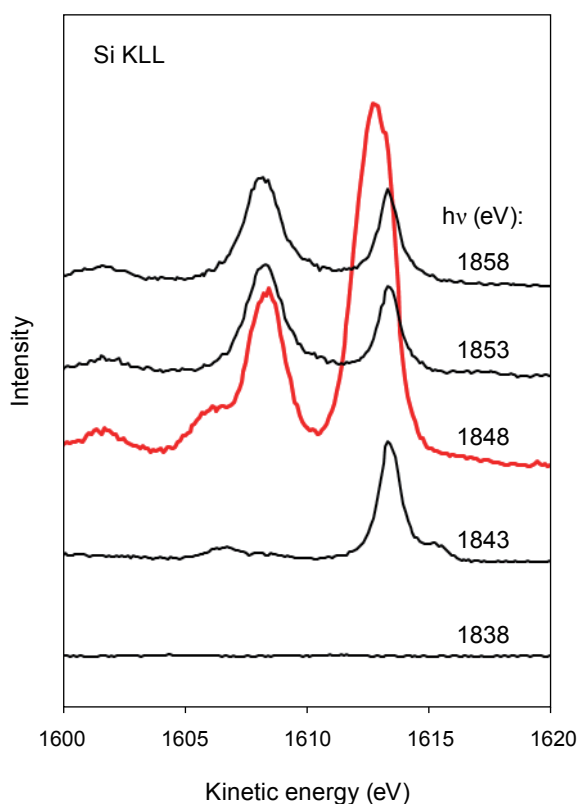


Fig. 5 Si KLL Auger spectra upon irradiation at photon energies of 1838, 1843, 1848 (thick, red), 1853 and 1858 eV.

indicating the resonant Auger peak of SiO₂.⁽²⁵⁾ Although this peak buried the SiC peak at the PE of 1848 eV, causing the XANES modification of SiC, the SiC peaks can be seen at PEs of 1853 eV and 1858 eV. This means that the resonant Auger peak could present only at the PE of the absorption edge of SiO₂. Consequently, it is expected that the influence of the resonant Auger peak is small in the EXAFS region.

For the SiC-side interface, the EXAFS oscillations and the Fourier transforms derived from the oscillations of SiC-selective DEY-EXAFS spectra are presented in **Fig. 6**, along with those of a bulk SiC sample for comparison. The EXAFS oscillations were extracted from each EXAFS spectrum shown in Fig. 4(a) using the ATHENA program as a function of the wave vector.⁽²⁶⁾ The Fourier transformation was performed

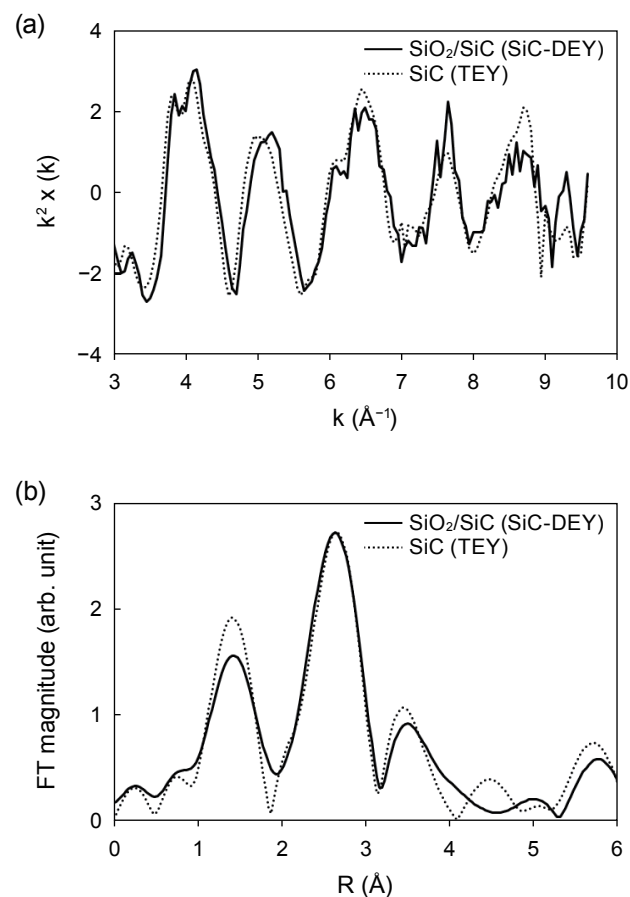


Fig. 6 (a) EXAFS oscillations extracted from the EXAFS spectra of the SiO₂/SiC interface (SiC-selective DEY) and SiC (TEY) (as a function of the wave vectors) and (b) Fourier transforms derived from the EXAFS oscillations (without considering phase shifts).

in the k range of 3–9 \AA^{-1} without consideration of phase shifts. The oscillations of the SiC-selective DEY spectrum were similar to those of the TEY spectrum for the bulk sample, indicating that the aforementioned influence of the resonant Auger was negligible, at least in the EXAFS region. The inelastic mean free path of electrons corresponding to the analysis depth was estimated to be approximately 4.2 nm using the TPP-2M formula.⁽²⁷⁾ Since the SiO₂ film thickness was 3.7 nm, the EXAFS spectrum of the SiC-side interface (probe depth < 1 nm) underneath the SiO₂ film could be nondestructively obtained. The intensity of the first-nearest-neighbor peak (1.3 \AA), corresponding to C atoms, for the SiO₂/SiC sample was 17% lower than that for the bulk SiC sample. Although compounds such as SiC_xO_y might be formed at the interface,^(3,28) they could not be detected because the position of the Auger peak would differ from that of the monitored SiC peak. Generally, the peak intensity of the Fourier transform depends on the coordination number. The second-nearest-neighbor peak for the SiO₂/SiC sample was in agreement with that for the bulk SiC sample, suggesting little structural disorder. Therefore, we propose that carbon vacancy defects could exist on the SiC side of the SiO₂/SiC interface. Moreover, conventional XPS measurements (PHI-Quantera SXM, X-ray: monochromatic AlK α , TOA: 45°) of the same samples showed that the carbon/silicon ratio of the SiC component in the SiO₂/SiC sample was less than 1 ($[\text{C}] < [\text{Si}]$), supporting the proposition that carbon vacancy defects could exist.

For the SiO₂-side interface, the EXAFS oscillations and the Fourier transforms derived from the oscillations of SiO₂-selective DEY-EXAFS spectra are presented in Fig. 7, along with those of the bulk SiO₂ sample for comparison. The oscillation extraction and Fourier transformation were conducted as in the case of SiC. The Fourier transform derived from the oscillations of the SiO₂-selective DEY-EXAFS spectrum differed slightly from that of the bulk SiO₂ sample in terms of atomic distance, the values of which were calculated without considering phase shifts. The first-nearest-neighbor distance was calculated via a fitting analysis using the ARTEMIS program,⁽²⁶⁾ and the phase shift and backward scattering factor values were calculated via FEFF.^(29,30) The fitting parameters used included the atomic distance, amplitude, and edge energy, whereas the Debye–Waller factor was fixed. The amplitude reduction factor was set to

0.992, which was determined from the TEY-EXAFS spectrum of the bulk SiO₂ sample. The obtained Si–O distance was 1.57 \AA with a reliability factor of 0.006. SiO₂ has various crystal structures such as quartz and cristobalite, and the Si–O distance varies around 1.6 \AA .⁽³¹⁾ The tridymite phase has the lowest density and the Si–O distance is the shortest, 1.53–1.56 \AA , which is close to our result (1.57 \AA). Ono and Saito reported that the tridymite-SiO₂/4H-SiC interface has the smallest lattice constant mismatch, although the SiC with Si-face.⁽³²⁾ The SiO₂ film investigated in this study includes the SiO₂/SiC interface, and the contribution of the interface to the measured spectra is relatively high because the thickness is quite thin. Hence, it is suggested that the SiO₂ side of the SiO₂/SiC interface could adopt a structure close to that of tridymite.

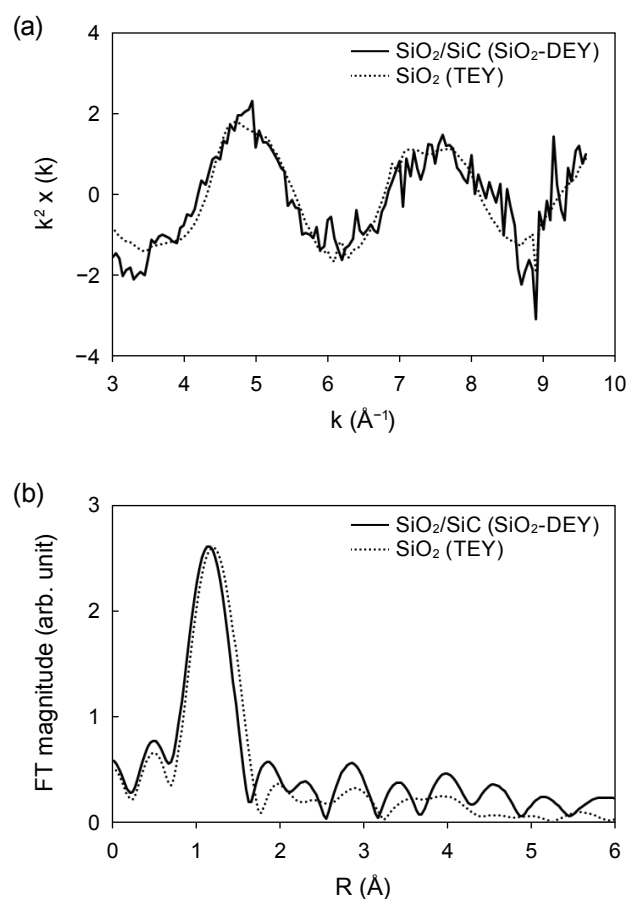


Fig. 7 (a) EXAFS oscillations extracted from the EXAFS spectra of the SiO₂/SiC interface (SiO₂-selective DEY) and SiO₂ (TEY) (as a function of the wave vectors) and (b) Fourier transforms derived from the EXAFS oscillations (without considering phase shifts).

4. Summary

We have reported on a local atomic structure analysis of the CVD-SiO₂/SiC(4H, m-face) interface, using a combination of chemical-state-selective EXAFS spectroscopy and a thinned SiO₂ film sample. The chemical-state-selective EXAFS measurements of SiO₂ and SiC were demonstrated by detection of bond-specific Auger electrons using the DEY mode. The Fourier transform derived from the SiC-selective DEY-EXAFS oscillations exhibited an intensity reduction (17%) of the first-nearest-neighbor peak with respect to the bulk SiC sample, suggesting that carbon vacancy defects could exist on the SiC side of the SiO₂/SiC interface. The Si–O distance determined from the SiO₂-selective DEY-EXAFS measurement was 1.57 Å, suggesting that the SiO₂ side could adopt a structure close to that of tridymite. The chemical-state-selective EXAFS method showed the availability of interface analysis for SiO₂/SiC and is expected to become a useful tool for the development of SiC-MOS devices.

Acknowledgments

The authors are grateful to Dr. Hiroshi Oji of Nagoya University Synchrotron Radiation Research Center, as well as Takaaki Murai and Dr. Toyokazu Nomoto of Aichi Synchrotron Radiation Center (AichiSR) for their contributions. The synchrotron radiation measurements were done at BL6N1 of AichiSR with the approval of Aichi Science and Technology Foundation (Experiments No. 201504061 and No. 201506019).

References

- (1) Tan, J., Das, M. K., Cooper Jr., J. A. and Melloch, M. R., *Appl. Phys. Lett.*, Vol. 70, No. 17 (1997), pp. 2280-2281.
- (2) Saks, N. S., Mani, S. S. and Agarwal, A. K., *Appl. Phys. Lett.*, Vol. 76, No. 16 (2000), pp. 2250-2252.
- (3) Kimoto, T., Kanzaki, Y., Noborio, M., Kawano, H. and Matsunami, H., *Jpn. J. Appl. Phys.*, Vol. 44, No. 3 (2005), pp. 1213-1218.
- (4) Okamoto, D., Yano, H., Hirata, K., Hatayama, T. and Fuyuki, T., *IEEE Electron Device Lett.*, Vol. 31, No. 7 (2010), pp. 710-712.
- (5) Di Ventura, M. and Pantelides, S. T., *Phys. Rev. Lett.*, Vol. 83, No. 8 (1999), pp. 1624-1627.
- (6) Chang, K. C., Nuhfer, N. T. and Porter, L. M., *Appl. Phys. Lett.*, Vol. 77, No. 14 (2000), pp. 2186-2188.
- (7) Buczko, R., Pennycook, S. J. and Pantelides, S. T., *Phys. Rev. Lett.*, Vol. 84, No. 5 (2000), pp. 943-946.
- (8) Cantin, J. L., von Bardeleben, H. J., Shishkin, Y., Ke, Y., Devaty, R. P. and Choyke, W. J., *Phys. Rev. Lett.*, Vol. 92, No. 1 (2004), 015502.
- (9) Ohnuma, T., Tsuchida, H. and Jikimoto, T., *Mater. Sci. Forum*, Vol. 457-460 (2004), pp. 1297-1300.
- (10) Knaup, J. M., Deák, P. and Frauenheim, T., *Phys. Rev. B*, Vol. 72 (2005), 115323.
- (11) Umeda, T., Esaki, K., Kosugi, R., Fukuda, K., Ohshima, T., Morishita, N. and Isoya, J., *Appl. Phys. Lett.*, Vol. 99 (2011), 142105.
- (12) Hatakeyama, T., Matsuhata, H., Suzuki, T., Shinohe, T. and Okumura, H., *Mater. Sci. Forum*, Vol. 679-680 (2011), pp. 330-333.
- (13) Watanabe, H., Hosoi, T., Kirino, T., Kagei, Y., Uenishi, Y., Chanthaphan, A., Yoshigoe, A., Teraoka, Y. and Shimura, T., *Appl. Phys. Lett.*, Vol. 99 (2011), 021907.
- (14) Hirai, H. and Kita, K., *Appl. Phys. Lett.*, Vol. 103 (2013), 132106.
- (15) Teo, B. K. and Joy, D. C., *EXAFS Spectroscopy* (1981), 275p., Plenum Press.
- (16) Isomura, N., Murai, T., Oji, H., Nomoto, T., Watanabe, Y. and Kimoto, Y., *Appl. Phys. Express*, Vol. 9 (2016), 101301.
- (17) Citrin, P. H., Eisenberger, P. and Hewitt, R. C., *Phys. Rev. Lett.*, Vol. 41, No. 5 (1978), pp. 309-312.
- (18) Brennan, S., Stöhr, J. and Jaegar, R., *Phys. Rev. B*, Vol. 24, No. 8 (1981), pp. 4871-4874.
- (19) Isomura, N., Murai, T., Oji, H., Nomoto, T., Watanabe, Y. and Kimoto, Y., *Jpn. J. Appl. Phys.*, Vol. 56 (2017), 081301.
- (20) Isomura, N., Kamada, M., Nonaka, T., Nakamura, E., Takano, T., Sugiyama, H. and Kimoto, Y., *J. Synchrotron Rad.*, Vol. 23, No. 1 (2016), pp. 281-285.
- (21) Yamamoto, M., Yoshida, T., Yamamoto, N., Yoshida, H. and Yagi, S., *e-J. Surf. Sci. Nanotech.*, Vol. 12 (2014), pp. 299-303.
- (22) Isomura, N., Soejima, N., Iwasaki, S., Nomoto, T., Murai, T. and Kimoto, Y., *Appl. Surf. Sci.*, Vol. 355 (2015), pp. 268-271.
- (23) Johansson, L. I., Virojanadara, C., Eickhoff, T. and Drube, W., *Surf. Sci.*, Vol. 529, No. 3 (2003), pp. 515-526.
- (24) Stöhr, J., *NEXAFS Spectroscopy* (1992), 403p., Springer.
- (25) Baba, Y., Yamamoto, H. and Sasaki, T. A., *Surf. Sci.*, Vol. 307-309, Part B (1994), pp. 896-900.
- (26) Ravel, B. and Newville, M., *J. Synchrotron Rad.*, Vol. 12, No. 4 (2005), pp. 537-541.
- (27) Tanuma, S., Powell, C. J. and Penn, D. R., *Surf. Interface Anal.*, Vol. 21, No. 3 (1994), pp. 165-176.
- (28) Radtke, C., Baumvol, I. J. R., Morais, J. and Stedile, F. C., *Appl. Phys. Lett.*, Vol. 78, No. 23 (2001), pp. 3601-3603.

- (29) Zabinsky, S. I., Rehr, J. J., Ankudinov, A., Albers, R. C. and Eller, M. J., *Phys. Rev. B*, Vol. 52, No. 4 (1995), pp. 2995-3009.
- (30) Ankudinov, A. L., Ravel, B., Rehr, J. J. and Conradson, S. D., *Phys. Rev. B*, Vol. 58, No. 12 (1998), pp. 7565-7576.
- (31) Gritsenko, V. A., *Phys.-Uspekhi*, Vol. 51, No. 7 (2008), pp. 699-708.
- (32) Ono, T. and Saito, S., *Appl. Phys. Lett.*, Vol. 106 (2015), 081601.

Figs. 2 and 3(a)

Reprinted from *Appl. Phys. Express*, Vol. 9 (2016), 101301, Isomura, N., Murai, T., Oji, H., Nomoto, T., Watanabe, Y. and Kimoto, Y., Local Atomic Structure Analysis of SiC Interface with Oxide Using Chemical-state-selective X-ray Absorption Spectroscopy, © 2016 The Japan Society of Applied Physics.

Figs. 3(b), 4, 5 and 7

Reprinted from *Jpn. J. Appl. Phys.*, Vol. 56 (2017), 081301, Isomura, N., Murai, T., Oji, H., Nomoto, T., Watanabe, Y. and Kimoto, Y., Chemical-state-selective X-ray Absorption Spectroscopy by Detecting Bond-specific Auger Electrons for SiO₂/SiC Interface, © 2017 The Japan Society of Applied Physics.

Noritake Isomura

Research Fields:

- Surface and Interface Analysis
- Materials Analysis Using Synchrotron Radiation

Academic Degree: Dr.Eng.

Academic Society:

- The Japan Society of Applied Physics



Takamasa Nonaka

Research Field:

- Materials Analysis Using Synchrotron Radiation

Academic Degree: Dr.Eng.

Academic Society:

- The Japanese Society for Synchrotron Radiation Research

Award:

- Promotion Award, The Ceramic Society of Japan, 2008



Yukihiko Watanabe

Research Field:

- Reliability Physics of MOS Devices

Academic Degree: Dr.Eng.

Academic Societies:

- IEEE Electron Device Society
- The Japan Society of Applied Physics

